Wave Loads on a Vertical Elastic Wall

Sheguang Zhang[1], Gaute Storhaug[1,2] & Dick K. P. Yue[1]

[1] Department of Ocean Engineering, MIT, Cambridge, MA 02139, USA

[2] The Norwegian Institute of Technology, Trondheim, Norway

(Abstract for the *10th International Workshop on Water Waves & Floating Bodies*, April 1995)

The deformation of an elastic structure may significantly modify the hydrodynamic loads on it. Kvålsvold & Faltinsen (1994) showed a drastic reduction in slamming loads on wetdecks when hydroelastic effect is considered. Zhang, Yue & Tanizawa (1995) recently found about 10% reduction in impact force on an elastic wall due to impact of a plunging breaker. The present study is aimed at a systematic numerical investigation on the hydroelastic effects on wave loads and hydrodynamic pressures on a vertical elastic wall due to three different loading conditions: sloshing of a standing wave in a wave tank; impact of a plunging breaker with air trapped between the breaker and the wall; and impingement of a plane fluid jet with a finite contact region.

For the fluid motion problem, we assume two-dimensional (fully-nonlinear) potential flow in a rectangular wave tank. The governing equation is Laplace's equation which is solved by a boundary integral method based on an application of Cauchy's integral theorem to the complex potential (Vinje & Brevig 1980). On the free surface of the fluid, fully nonlinear boundary conditions are imposed and integrated following Lagrangian points. The elastic wall is modeled as an elementary cantilever beam and represented in terms its dry mode eigenfunctions. The dynamic equation for the modal amplitudes is solved using the Newmark–β method (*e.g.*, Bathe & Wilson 1976). The coupling between the fluid and the beam is implemented such that at each time step, the fluid motion is determined by solving the boundary value problem with the normal velocity on the fluid-wall interface specified by the velocity of the wall. The hydrodynamic pressure on the wall can then be calculated and imposed as a beam loading to move the wall to a new position at the next time step. The response of the wall is obtained and its velocity is fed back to the fluid and the process is repeated.

Two issues related to the numerical scheme are addressed. One concerns the initial condition to start the calculation. Since the wall is elastic and at rest initially, the initial pressure distribution of the fluid on the wall has to be determined by a relation that balances the pressure with the inertia of the wall at $t = 0$ (Duncan & Zhang 1991). The other issue is related to the stability of the numerical time integration and involves the introduction of a generalized (instantaneous for the actual free-surface profile) modal added mass. This makes it possible to simulate strong interaction cases such as one in which the wall is relatively soft and light. Figure 1 shows a sample time history of the stable (with the added mass) and unstable (without using the added mass) simulations for such a case.

In this coupled system, the time scales for characterizing the fluid motion, the effect of

the trapped air (for the case of the plunger impact), and the response of the beam are proportional to $(h_0/g)^{1/2}$, $h_0(\rho/P_0)^{1/2}$ and $L^2(M/EI)^{1/2}$, respectively. Here ρ is the density of the fluid; g, the gravity acceleration; h_0, the initial water depth; P_0, initial air pressure in the air pocket; L, the length of the beam; M, the mass of the beam per unit area; E, the elastic modulus; and I, the second moment of area of the cross-section of the beam, respectively. For simplicity, time, length and mass units have been chosen so that ρ, g and h_0 are unity.

For the case of standing wave sloshing in the rectangular tank with an elastic end wall, figure 2 presents the ratio of the force increase on the elastic wall relative a rigid wall. Here T_1 $(= 1.78L^2(M/EI)^{1/2}/(h_0/g)^{1/2})$ is the non-dimensional first-mode natural period of the beam, and the beam mass M is varied. The standing wave (linear) frequency is $\approx$0.9. It is seen that the force reduction due to hydroelasticity depends strongly on M but is not sensitive to the change of T_1 for $T_1 > 5$. The pressure change at the middle of the beam length is shown in figure 3, which shows a similar dependency on M as the forces in figure 2.

The hydroelastic effect becomes more complicated when an additional time scale is involved such as that introduced by a trapped air pocket. This is the case of the impact of a plunging breaker wave with air trapping we consider (see Zhang, et al. 1995 for details). As an example, figure 4 plots the total force (above the still water level) for the rigid and elastic cases. The maximum impact force reduction due to the hydroelastic effect can be as large as 20%. Preliminary results indicate that within a wide range of practical EI values, the mass per unit area of the beam M is the dominant factor in determining the effect of hydroelasticity on the wave-induced loads.

Finally, we consider the case of the impact of a water jet with finite contact width such as the relatively flat portion of a wave front. Unlike the earlier examples, extremely high impact pressures are expected and local hydroelastic effects become critial. Compressibility of the fluid also needs to be considered to capture the high acoustic impact pressure at the initial stage of the impact. The analysis here is somewhat analogous to that in Kvålsvold & Faltinsen (1994) and will be presented at the workshop.

References

Bathe, K. J. & Wilson, E. L. 1976 *Numerical Methods in Finite Element Analysis.* Prentice Hall.

Duncan, J. H. & Zhang, S. 1991 Numerical calculations of the growth and collapse of a vapor cavity in the vicinity of a compliant wall. *Mathematical Approaches in Hydrodynamics* (Ed. Miloh), SIAM.

Kvålsvold, J. & Faltinsen, O. M. 1994 Slamming loads on wetdecks of multihull vessels. *Proc. Int. Conf. Hydroelasticity in Marine Technology, Trondheim, Norway.* (Ed. Faltinsen), pp. 205–220.

Vinje, T. & Brevig, P. 1980 Numerical simulation of breaking waves. *3rd Int. Conf. on Finite Elements in Water Resources*, Univ. of Miss., Oxford, Miss., USA.

Zhang, S., Yue, D. K. P. & Tanizawa, K. 1995 The impact of a breaking wave on a vertical wall. *J. Fluid Mech.* (submitted).

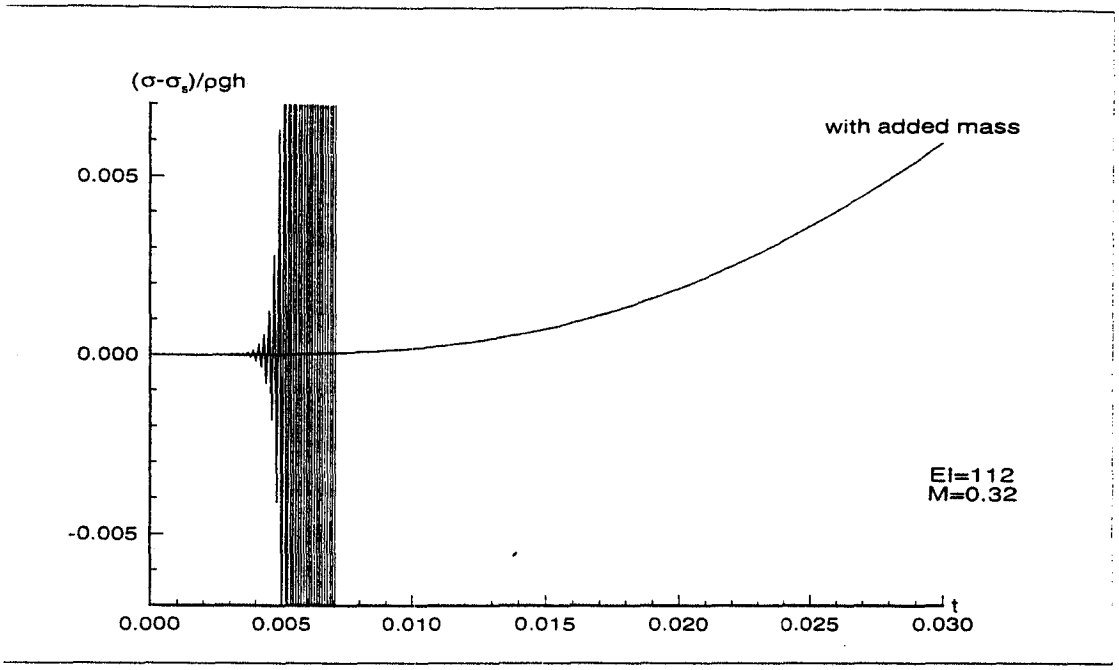

Figure 1: Stress calculation with the generalized added mass (smooth curve) and without the add mass (oscillating curve) versus time. The first-mode modal mass is 0.096 and the first-mode added modal mass is 0.08.

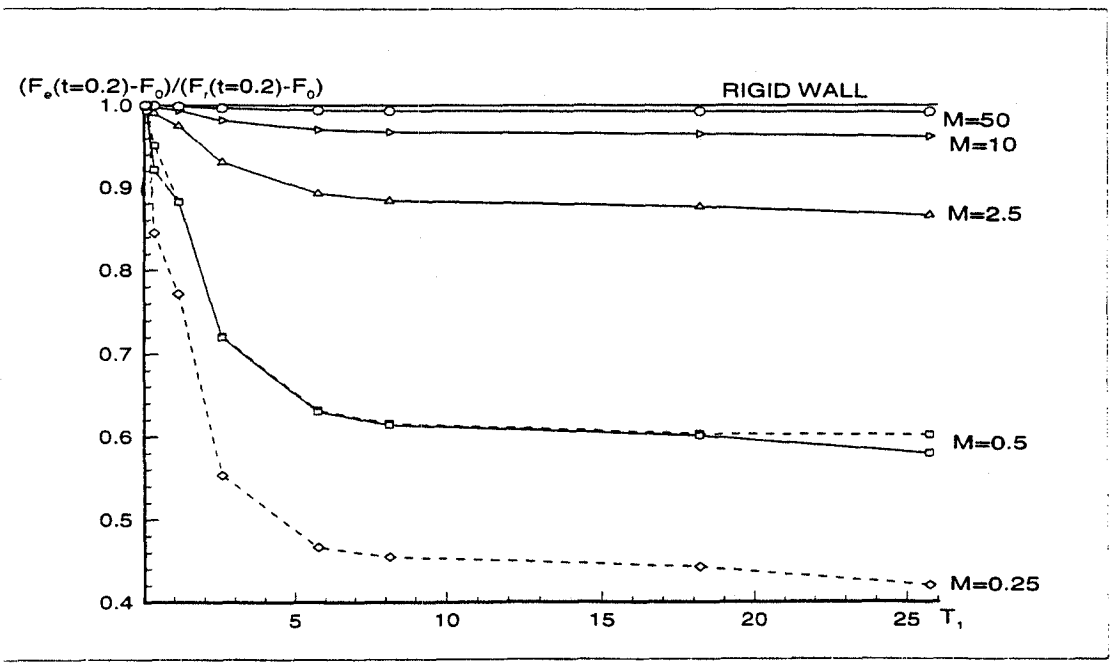

Figure 2: The ratio of the change of the forces on the elastic walls to the change of the force on a rigid wall as the function of the first eigenperiod T_1. F_0 is the force on the wall at $t = 0$. The dashed lines are the results obtained with the generalized added mass.

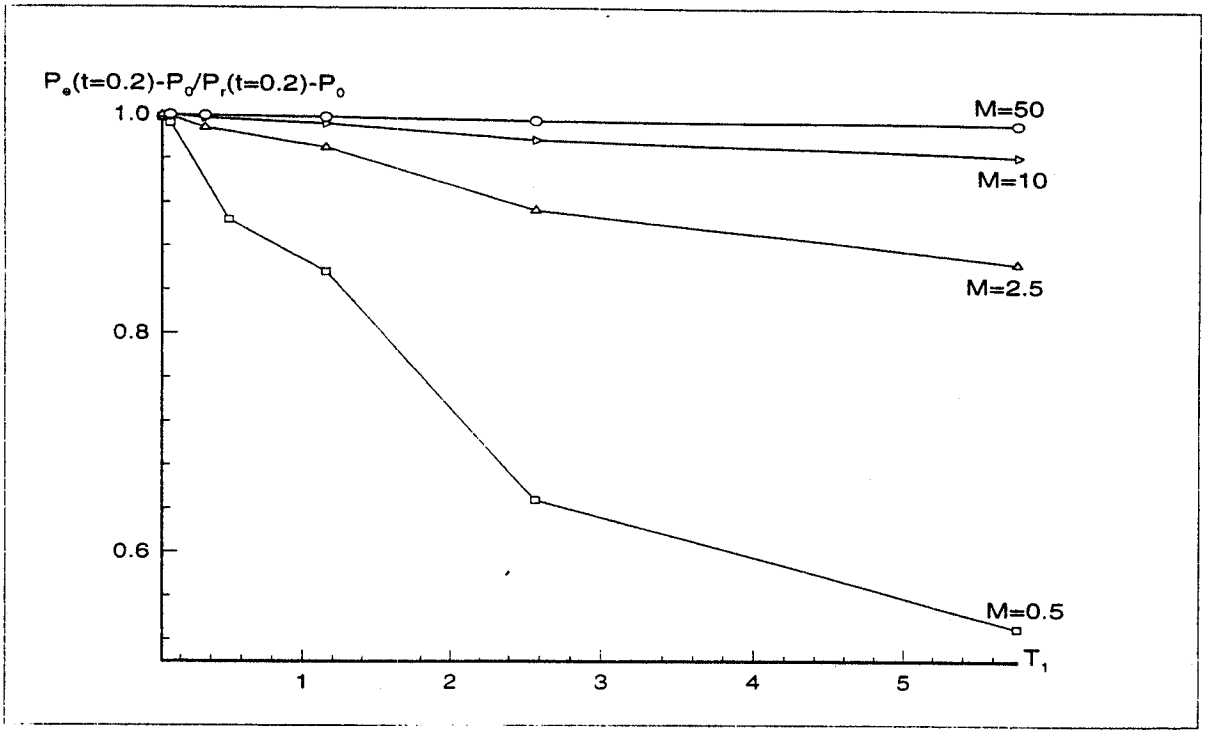

Figure 3: The ratio of the change of the pressures at a fixed point on the elastic walls to the change of the pressure at the same point on a rigid wall as the function of the first eigenperiod. P_0 denotes the pressure at the fixed point at $t = 0$.

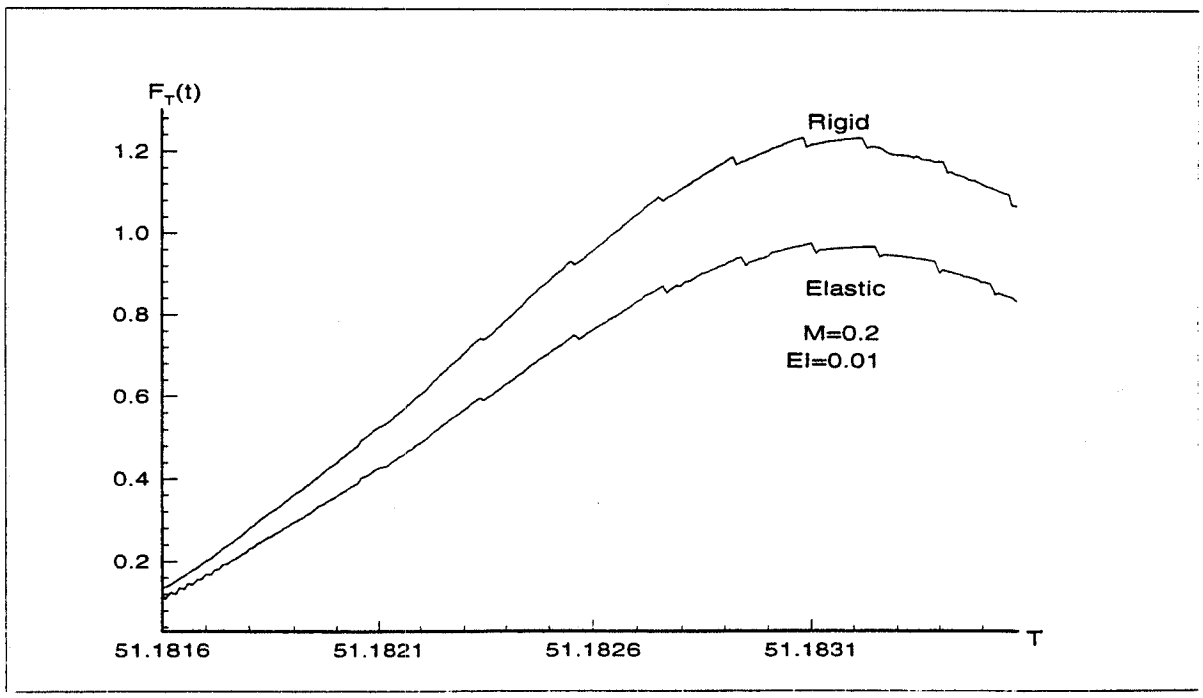

Figure 4: Total force on an elastic wall with $M = 0.2$ and $EI = 0.01$ and on a rigid wall versus time. The total forces are the summation of the pressure distributions on the walls above the still water lever.